Synthesis and Characterization of a Series of $CpW(CO)_2PR_3H$, $[CpW(CO)_2PR_3]^-$, $[CpW(CO)_2PR_3(CH_3CN)]^+$, and $[CpW(CO)_2PR_3]_2$ Complexes

*Diane P. Isaacs and Jillian L. Dempsey**

Department of Chemistry, University of North Carolina at Chapel Hill, Chapel Hill, North Carolina 27599-3290, United States

Key words: Metal hydrides, thermochemistry, pK_a

Abstract

A series of tungsten cyclopentadienyl carbonyl complexes were prepared and characterized to quantify their thermochemical properties and explore their reactivity. The PR_3 ligand was systematically varied across a series of $CpW(CO)_2PR_3H$ metal hydride complexes, where PR_3 = $P(OEt)_3$, $P(Bu)_3$, and $P(Cy)_3$. These complexes are known to undergo multiple proton, electron, and proton-coupled electron transfer reactions to access a variety of species including $[CpW(CO)_2PR_3]^-$, $[CpW(CO)_2PR_3(CH_3CN)]^+$, and $[CpW(CO)_2PR_3]_2$. Cyclic voltammograms of the $CpW(CO)_2PR_3H^{\bullet+/0}$ and $[CpW(CO)_2PR_3]^{\bullet 0/-}$ couples are chemically irreversible, indicating chemical reactivity upon oxidation; the anodic peak potential shifts to lower potentials as the donating ability of phosphine is increased, agreeing with previous literature on similar complexes. Additionally, voltammograms of $[CpW(CO)_2P(Cy)_3]^-$ become chemically reversible at scan rates above 500 mV/s, indicating that the dimerization of the $[CpW(CO)_2PR_3]^\bullet$ product, formed by the oxidation of $[CpW(CO)_2PR_3]^-$, is slower with the sterically bulky phosphine $P(Cy)_3$, and at high

scan rates the species can be reduced before dimerization occurs. Further, as the donating ability of the phosphine increases, the pK_a of the $CpW(CO)_2PR_3H$ complexes increases. This work shows how ligand sterics and electronics can tune the thermochemical properties that underpin proton, electron, and proton-coupled electron transfer reactivity of these complexes.

Introduction

Transition metal hydride complexes are key intermediates in many fuel forming reactions including CO_2 reduction, H^+ reduction, N_2 reduction, and H_2 oxidation.[1–4] It is important to understand the proton–coupled electron transfer (PCET) reactivity of transition metal hydride complexes, as the formation and reactivity of metal hydride species can generate a range of species and reactive intermediates.[5–7] Notably, the isolation and characterization of PCET intermediates can enable analysis of the more complicated reactions as a whole.

$CpW(CO)_2LH$ (Cp = cyclopentadienyl, L = Lewis base) complexes[5,6,8,9] are a well-studied class of transition metal hydride complexes.[5–7,10–13] These transition metal hydride complexes are known to undergo deprotonation reactions to yield $[CpW(CO)_2L]^-$,[5–7] oxidation reactions coupled with a PCET event and solvent (acetonitrile) binding to form $[CpW(CO)_2L(CH_3CN)]^+$,[5–7,14] and a proton-coupled electron transfer reaction to yield $[CpW(CO)_2L]^\bullet$, which can dimerize to form

$[CpW(CO)_2L]_2$ or undergo disproportionation (and solvent ligation) to form $[CpW(CO)_2L(CH_3CN)]^+$ and $[CpW(CO)_2L]^-$(Scheme 1).[5–7,11,14–17]

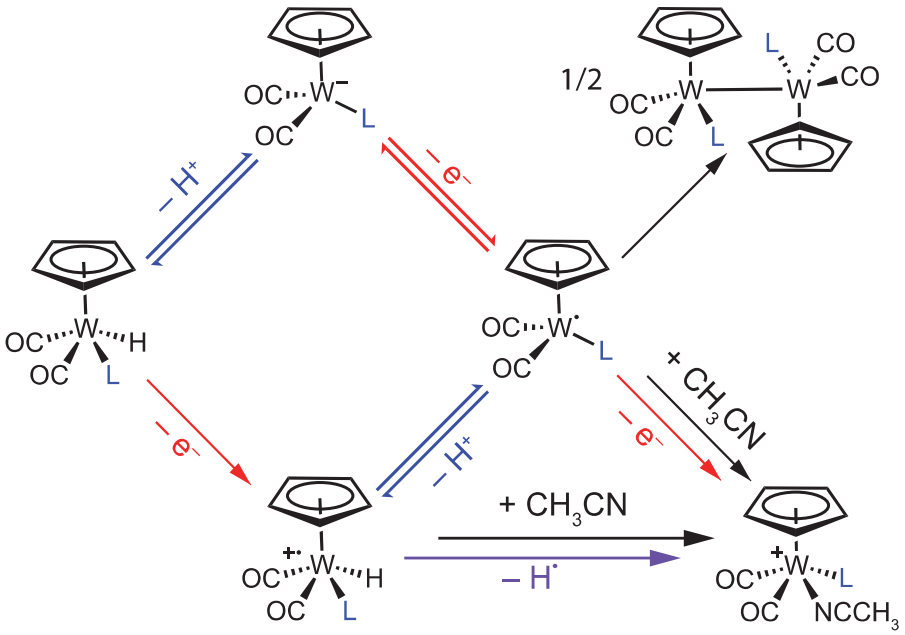

Scheme 1: Reaction scheme depicting the thermochemical and chemical steps between $CpW(CO)_2LH$, $[CpW(CO)_2L]^-$, $[CpW(CO)_2L(CH_3CN)]^+$, and $[CpW(CO)_2L]_2$. Red arrows represent electron transfer, blue arrows represent proton transfer, purple arrows represent hydrogen atom transfer, and black arrows represent chemical steps.

$CpW(CO)_2LH$ complexes can be synthesized with a variety of Lewis base ligands (L), ranging from carbonyls to carbenes to phosphines.[5,6,10,18] The steric and electronic properties of L can be systematically changed, and the influence of L on the thermochemical properties and reactivity of $CpW(CO)_2LH$ can be interrogated. Ligands such as monodentate trialkyl or triaryl phosphines (PR_3) offer an accessible spectrum of electronic and steric properties. For instance, the electronic properties of PR_3 ligands have been well studied by Tolman[19] and their steric bulk can be readily quantified by the Tolman cone angle.[20,21] Some $CpW(CO)_2(PR_3)H$ complexes have been studied previously,[5,10,13] however other derivatives only been mentioned in passing or have not yet reported, such as PR_3 = $P(OEt)_3$, $P(Bu)_3$, or $P(Cy)_3$ ($P(OEt)_3$ = triethyl phosphite, $P(Bu)_3$ =

tributyl phosphine, and $P(Cy)_3$ = tricyclohexyl phosphine).[18,22] In this work, we report the synthesis and thermochemical properties of a family of $CpW(CO)_2PR_3H$ complexes with PR_3 = $P(OEt)_3$, $P(Bu)_3$, and $P(Cy)_3$. We also report the synthesis and characterization of related species, $[CpW(CO)_2PR_3]^-$, $[CpW(CO)_2PR_3(CH_3CN)]^+$, and $[CpW(CO)_2PR_3]_2$, which are products of proton, electron, and proton-coupled electron transfer reactions. Through comprehensive characterization, we reveal how the electronics and sterics of these different phosphine ligands affect thermochemical properties and the kinetics of their reactivity, augmenting existing datasets for related complexes and strengthening trends for this important class of molecules.

Experimental

General considerations

All syntheses and analyses were performed under a nitrogen atmosphere, either in an inert atmosphere glovebox or on a Schlenk line, unless otherwise specified. Synthesis of $CpW(CO)_3H$[23,24] and triphenylmethyl radical[25] (Moses Gomberg's dimer) were synthesized according to literature procedures. Triethyl phosphite and tricyclohexylphosphine was purchased from Fisher Scientific. Tributyl phospine was purchased from SigmaAldrich. Acetonitrile (Fisher Scientific, HPLC grade, >99.9%), diethyl ether (Fisher Scientific, >99%), and pentane (Fischer Scientific, >99%) were degassed with argon and dried using a Pure Process Technology solvent system. Deuterated acetonitrile (Cambridge Isotope Laboratories, >99.8%) was stirred over CaH_2 for 24 hours, degassed using a freeze–pump–thaw technique, vacuum transferred to a Strauss flask, and stored under an inert-atmosphere glovebox. All NMR spectra were recorded on either a Bruker NEO 400 MHz spectrometer with Prodigy probe, a Bruker AVIII 500 MHz spectrometer with a standard 5 mm broad band probe, or a Bruker B600 MHz spectrometer with a BBFO probe. UV–

visible absorbance measurements were recorded on an Agilent Cary 60 UV–vis spectrophotometer using 1 cm path length quartz cuvettes. Infrared spectra were acquired on Thermo Scientific Nicolet iS5 FT-IR spectrometer utilizing an air-tight solution cell. High-resolution mass spectrometry was collected with a Thermo Scientific Q Exactive HF-X instrument.

Electrochemistry. Electrochemical measurements were performed in a nitrogen-filled glovebox at room temperature with a WaveDriver potentiostat (Pine Research) using a glassy carbon working electrode, a glassy carbon counter electrode, and a silver wire pseudo-reference electrode. The pseudo-reference silver wire electrode was submerged in a glass tube containing electrolyte (0.25 M $[Bu_4N][PF_6]$ in CH_3CN) and separated from the solution with a porous glass Vycor tip. The electrochemical cell used was a 20 mL scintillation vial fitted with a custom-made Teflon cap for the three electrodes. The electrode leads in the glovebox were connected to the WaveDriver with a custom shielded electrode cable feedthrough. All scans were internally referenced to the ferrocenium/ferrocene couple (0 V vs. $Fc^{+/0}$). Ohmic drop was minimized using a high electrolyte concentration (0.25 M $[Bu_4N][PF_6]$), as well as by minimizing the distance between the working and reference electrodes. The positive feedback R_u method (Pine Research) was used to compensate for the residual ohmic drop. Glassy carbon electrodes (CH Instruments) were polished with 0.05 μm alumina powder (CH Instruments, contained no agglomerating agents) Milli-Q water slurries, rinsed, and ultrasonicated briefly in Milli-Q water to remove residual polishing powder. The working electrode was pretreated with cyclical scans from approximately 1 to −2.5 V at 200 mV/s in 0.25 M $[Bu_4N][PF_6]$ in CH_3CN until cycles were superimposable.

Synthesis of $CpW(CO)_2PR_3H$

$CpW(CO)_2P(OEt)_3H$. Preparation of $CpW(CO)_2P(OEt)_3H$ was adapted from literature procedures of similar complexes.[5,13,23,24] In an inert atmosphere glovebox, triethyl phosphite (0.217 mL, 1.27

mmol, 1.6 equiv) and $CpW(CO)_3H$ (0.2679 g, 0.805 mmol, 1 equiv, yellow solid) were added to a 20 mL scintillation charged with a stir bar. To the vial, 5 mL of toluene was added. The reaction was stirred for 18 hrs at room temperature. Toluene was removed under vacuum to yield a yellow oil. The oil was dissolved in 2 mL pentane and placed in the freezer. After 1 day, a light-yellow solid crashed out of solution. Pentane was decanted off with a pipette and the solid was rinsed with cold pentane three times. The yellow solid was then dried under vacuum (0.2432 g, 0.515mmol, 64% yield) and stored in the glovebox freezer. ^{1}H NMR (400 MHz, CD_3CN) **δ** 5.39 (5H, s), 3.43 (6H, m), 1.23 (9H, t, J = 14.0, 7.0 Hz), – 8.25 (1H, d, $^2J^{31}_{P-H}$ = 72.0 Hz) ^{31}P NMR (162 MHz, CD_3CN) **δ** 153 (1P, s $^1J^{183}_{W-P}$ = 425 Hz). IR in pentane 1955 and 1885 cm^{-1} (CO). IR in CH_2Cl_2 1941 and 1855 cm^{-1} (CO). Anal. Calcd for $C_{13}H_{21}O_5PW$: C, 33.07; H, 4.49; N, 0. Found C, 33.01; H, 4.41; N, 0. HRMS (ESI-HFX) m/z: $[M + H]^+$ Calcd for $C_{13}H_{21}O_5PWH$ 473.115; Found 473.071.

$CpW(CO)_2P(Bu)_3H$. Preparation of $CpW(CO)_2(P(Bu)_3H$ was adapted from literature procedures of similar complexes.[5,13,23,24] In an inert atmosphere glovebox, tributylphosphine (0.0747 mL, 0.3028 mmol, 1 equiv, yellow solid) and $CpW(CO)_3H$ (0.1010 g, 0.3034 mmol, 1 equiv) were added to a scintillation vial charged with a stir bar. To the vial, 5 mL of pentane was added. The reaction was stirred for 18 hrs at room temperature. Unlike other analogs, $CpW(CO)_2(P(Bu)_3H$ did not crash out of pentane and a stoichiometric ratio of $CpW(CO)_3H$ and PR_3 were required to isolate the product. The pentane was removed under vacuum and a yellow oily solid was collected (0.1441 g, 0.2835 mmol, 93 % yield) and stored in the glovebox freezer. ^{1}H NMR (400 MHz, CD_3CN) **δ** 5.35 (5H, s, Cis), 5.17 (5H, s, Trans), 1.73 (6H, m), 1.37 (12 H, m), 0.92 (9H, t, J = 14.1, 6.8 Hz), -8.00 (1H, d, Cis, $^2J^{31}_{P-H}$ = 65.2 Hz. $^1J^{183}_{W-H}$ = 48.4 Hz), – 8.22 (1H, d, Trans, $^2J^{31}_{P-H}$ = 23.0 Hz) 72% Cis isomer, 28 % Trans isomer. ^{31}P NMR (162 MHz, CD_3CN) **δ** 14.1 (1P, s , Cis, $^1J^{183}_{W-P}$ = 254 Hz), 7.36 (1P, s, Trans, $^1J^{183}_{W-P}$ = 279 Hz). IR in pentane 1939 and 1856 cm^{-1} (CO). IR in

CH_2Cl_2 1918 and 1830 cm^{-1} (CO). Anal. Calcd for $C_{19}H_{33}O_2PW$: C, 44.89; H, 6.57; N, 0. Found C, 45.19; H, 6.56; N, 0. HRMS (ESI-HFX) m/z: $[M + H]^+$ Calcd for $C_{19}H_{33}O_2PWH$ 509.256; Found 509.180.

$CpW(CO)_2P(Cy)_3H$. Preparation of $CpW(CO)_2(PCy)_3H$ was adapted from literature procedures of similar complexes.[5,13,23,24] In an inert atmosphere glovebox, tricyclohexylphosphine (0.1239 g, 0.4418 mmol, 1 equiv) and $CpW(CO)_3H$ (0.1640 g, 0.4926 mmol, 1.11 equiv, yellow solid) were added to a scintillation vial charged with a stir bar. To the vial, 3 mL of pentane was added. The reaction was stirred for 72 hrs at room temperature. A light-yellow solid crashed out slowly over time. The yellow solid was collected by filtration and rinsed with pentane 3 times (0.1647 g, 0.2809 mmol, 64% yield). ^1H NMR (400 MHz, CD_3CN) **δ** 5.36 (5H, s), 1.84 (12H, m), 1.67 (6H, m), 1.27 (15H, m), – 7.64 (1H, d, $^2J^{31}_{P-H}$ = 60.9 Hz)). ^{31}P NMR (162 MHz, CD_3CN) **δ** 43.2 (1P, s). IR in pentane 1934 and 1848 cm^{-1} (CO). IR in CH_2Cl_2 1941 and 1856 cm^{-1} (CO). Anal. Calcd for $C_{25}H_{39}O_2PW$: C, 51.20; H, 6.72; N, 0. Found C, 50.56; H, 6.35; N, 0. HRMS (ESI-HFX) m/z: $[M + H]^+$ Calcd for $C_{25}H_{39}O_2PWH$ 587.382; Found 587.227.

Synthesis of $Na[CpW(CO)_2PR_3]$

$Na[CpW(CO)_2P(OEt)_3]$. Preparation of $Na[CpW(CO)_2P(OEt)_3]$ was adapted from literature procedures of similar complexes. [5,16] In an inert atmosphere glovebox $CpW(CO)_2P(OEt)_3H$ (0.0514 g, 0.109 mmol, 1 equiv) was combined with NaH (0.0029 g, 0.12 mmol, 1.1 equiv) in a 20 mL scintillation vial. The solids were then dissolved in 5 mL acetonitrile and stirred overnight. The solution was filtered to remove excess NaH and solvent was removed under vacuum to yield a yellow solid (0.0550 g, 0.0111 mmol, 101%). ^1H NMR (400 MHz, CD_3CN) **δ** 4.84 (5H, s), 3.78 (6H, m), 1.13 (9H, t, J = 14.1, 7.1 Hz). ^{31}P NMR (162 MHz, CD_3CN) **δ** 177 (1P, s, $^1J^{183}_{W-P}$ = 701

Hz). IR in CH_2Cl_2 1942 and 1848 cm^{-1} (CO). HRMS (ESI-HFX) m/z: [M^-] Calcd for $C_{13}H_{21}O_5PW$ 471.099; Found 471.057.

Na[CpW(CO)$_2$P(Bu)$_3$]. Preparation of Na[CpW(CO)$_2$P(Bu)$_3$] was adapted from literature procedures of similar complexes. [5,16] In an inert atmosphere glovebox CpW(CO)$_2$P(Bu)$_3$H (0.0510 g, 0.101 mmol, 1 equiv) was combined with NaH (0.0028 g, 0.12 mmol, 1.2 equiv) in a scintillation vial. The solids were dissolved in 5 mL acetonitrile and stirred overnight. The solution was filtered to remove excess NaH and the solvent removed under vacuum to yield a yellow solid (0.0501 g, 0.0946 mmol, 94/%). ^{1}H NMR (400 MHz, CD_3CN) **δ** 4.70 (5H, s), 1.58 (6H, m), 1.34 (12H, m), 0.90 (9H, t, J = 14.3, 7.2 Hz). ^{31}P NMR (162 MHz, CD_3CN) **δ** 21.6 (1P, s, $^1J^{183}_{W-P}$ = 458 Hz). IR in CH_2Cl_2 1937 and 1844 cm^{-1} (CO). HRMS (ESI-HFX) m/z: [M^-] Calcd for for $C_{19}H_{32}O_2PW$ 507.240; Found 507.166.

Na[CpW(CO)$_2$P(Cy)$_3$]. Preparation of Na[CpW(CO)$_2$P(Cy)$_3$] was adapted from literature procedures of similar complexes. [5,16] In an inert atmosphere glovebox CpW(CO)$_2$P(Cy)$_3$H (0.0345 g, 0.0589 mmol, 1.1 equiv) was combined with NaH (0.0014 g, 0.058, 1 equiv)in a scintillation vial. The solids were dissolved in 10 mL acetonitrile and stirred overnight. The solution was filtered to remove excess NaH and the solvent removed under vacuum to yield a yellow solid (0.0347 g, 0.0570 mmol, 98%). ^{1}H NMR (400 MHz, CD_3CN) **δ** 4.70 (5H, s), 1.78 (18H, m), 1.20 (15H, m). ^{31}P NMR (162 MHz, CD_3CN) **δ** 43.1 (1P, s, $^1J^{183}_{W-P}$ = 452 Hz). IR in CH_2Cl_2 1937 and 1848 cm^{-1} (CO). HRMS (ESI-HFX) m/z: [M^-] Calcd for for $C_{25}H_{38}O_2PW$ 585.366; Found 585.214.

Synthesis of [CpW(CO)$_2$PR$_3$(CH$_3$CN)][PF$_6$]

[CpW(CO)$_2$P(OEt)$_3$(CH$_3$CN)][PF$_6$]. Preparation of [CpW(CO)$_2$P(OEt)$_3$(CH$_3$CN)][PF$_6$] was adapted from literature procedures of similar complexes.[11,14,24,26] In an inert atmosphere glovebox,

$CpW(CO)_2P(OEt)_3H$ (0.0490 g, 0.104 mmol, 1.07 equiv) was added to a 20 mL scintillation vial. The solid was dissolved in 1 mL dichloromethane and 5 equivalents of acetonitrile (26 μL) was added. Trityl hexafluorophosphate (0.0377 g, 0.0971 mmol, 1 equiv) was added to a 20 mL scintillation vial and dissolved in 2 mL dichloromethane. The trityl PF_6 solution was added to the, $CpW(CO)_2P(OEt)_3H$ solution while stirring The solution was stirred for 15 mins at room temperature while shielded from light. The solution turned an orange/red color within a couple of minutes. The solvent was removed by vacuum while shielding the vial from light to yield an orange/red solid. Diethyl ether was added to the vial to yield orange solution with undissolved red/orange solid. The orange diethyl ether solution decanted off and the solid was dried under vacuum to afford a red/orange solid (0.0507g, 0.0793 mmol, 82%). ^{1}H NMR (400 MHz, CD_3CN) **δ** 5.59 (5H, s), 4.05 (2H, m), 2.52 (3H, s), 1.31 (3H, t, J = 14.1, 7.1 Hz). ^{31}P NMR (162 MHz, CD_3CN) **δ** 131.77 (1P, s, $^1J^{183}_{W-P}$ = 347 Hz), -144.64 (1P, septet, PF_6). IR in CH_2Cl_2 1912 and 1998 cm^{-1} (CO). Anal. Calcd for $C_{15}H_{23}O_5NP_2WF_6$: C, 27.41; H, 3.53; N, 2.13. Found C, 27.59; H, 3.38; N, 2.03. HRMS (ESI-HFX) m/z: $[M]^+$ Calcd for $C_{15}H_{23}O_5NPW$ 512.153; Found 512.082.

$[CpW(CO)_2P(Bu)_3(CH_3CN)][PF_6]$. Preparation of $[CpW(CO)_2P(Bu)_3(CH_3CN)][PF_6]$ was adapted from literature procedures of similar complexes.[11,14,24,26] In an inert atmosphere glovebox, $CpW(CO)_2P(Bu)_3H$ (0.0491 g, 0.0968 mmol, 1 equiv) and trityl hexafluorophosphate (0.0375 g, 0.0966 mmol, 1 equiv) were added to a 20 mL scintillation vial. The solids were dissolved in 5 mL dichloromethane and 5 equivalents of acetonitrile (26 μL) were added. The solution was stirred for 20 mins at room temperature. The solvent was removed by vacuum while shielding the vial from light. Diethyl ether was added to the vial to yield red solution with undissolved orange solid. The red diethyl ether solution was decanted. The orange solid rinsed with ether 3 times and dried under vacuum (0.0359g, 0.0518 mmol, 53%). ^{1}H NMR (400 MHz, CD_3CN) **δ** 5.80 (5H, s), 2.56

(3H, s), 1.91 (6H, m), 1.41 (12H, m), 0.95 (9H, t, J = 13.9, 6.8 Hz). ^{31}P NMR (162 MHz, CD_3CN) **δ** – 0.42 (1P, s, $^{1}J^{183}_{W-P}$ = 235 Hz), **δ** –145 (1P, septet, PF_6). IR CH_2Cl_2 in, 1889 and 1971 cm $^{-1}$ (CO). Anal. Calcd for $C_{21}H_{35}O_2NP_2WF_6$: C, 36.38; H, 5.10; N, 2.02. Found C, 36.38; H, 5.09; N, 1.91. HRMS (ESI-HFX) m/z: $[M]^+$ Calcd for $C_{21}H_{35}O_2NPW$ 547.286; Found 547.219.

[CpW(CO)$_2$P(Cy)$_3$(CH$_3$CN)][PF$_6$]. Preparation of [CpW(CO)$_2$P(Cy)$_3$(CH$_3$CN)][PF$_6$] was adapted from literature procedures of similar complexes.[11,14,24,26] In an inert atmosphere glovebox, CpW(CO)$_2$P(Cy)$_3$H (0.0581 g, 0.0990 mmol, 1.04 equiv) and trityl hexafluorophosphate (0.0370 g, 0.0953 mmol, 1 equiv) were added to a 20 mL scintillation vial. Solids were dissolved in 5 mL dichloromethane and 5 equivalents of acetonitrile (26 μL) were added. The solution was stirred for 10 mins at room temperature. The solvent was removed by vacuum while shielding the vial from light. Diethyl ether was added to the vial to yield red solution with an undissolved orange solid. The red diethyl ether solution was decanted. The orange solid was rinsed with ether 3 times and dried under vacuum (0.0651 g, 00844 mmol, 89%). ^{1}H NMR (400 MHz, CD_3CN)) **δ** 5.86 (5H, s), 2.56 (3H, s), 1.84 (12H, m), 1.73 (3H, m) 1.43 (6H, m), 1.31 (12H, m). ^{31}P NMR (162 MHz, CD_3CN) **δ** 21.1 (1P, s, $^{1}J^{183}_{W-P}$ = 242 Hz), – 145 (1P, septet, PF_6). IR in CH_2Cl_2 1912 and 1998 cm^{-1} (CO). Anal. Calcd for $C_{27}H_{41}O_2NP_2WF_6$: C, 42.03; H, 5.37; N, 1.82. Found C, 42.36; H, 5.44; N, 1.61. HRMS (ESI-HFX) m/z: $[M]^+$ Calcd for $C_{27}H_{41}O_2NPW$ 626.420; Found 626.238.

Synthesis of [CpW(CO)$_2$PR$_3$]$_2$

[CpW(CO)$_2$P(OEt)$_3$]$_2$. Preparation of [CpW(CO)$_2$P(OEt)$_3$]$_2$ was adapted from literature procedures of similar complexes.[14,15,24,27] In an inert atmosphere glovebox, CpW(CO)$_2$P(OEt)$_3$H (0.0530 g, 0.112 mmol, 2 equiv) and (Ph$_3$C)$_2$ (0.0246 g, 0.0505 mmol, 1 equiv) were combined in a 20 mL scintillation vial. The solids were then dissolved in 3 mL diethyl ether and stirred for 10 min at room temperature. The solvent was removed under vacuum, rinsed 3 times with pentane,

and dried under vacuum for 30 mins to yield a red solid (0.0103 g, 0.0110 mmol, 22%). ^{1}H NMR (400 MHz, CD_3CN) **δ** 5.13 (10H, s, gauche), 5.05 (10H, s, anti), 4.00 (12H, m), 1.29 (18H, t, *J* = 14.0, 7.1 Hz, gauche), 1.25 (18H, t, *J* = 14.1, 7.1 Hz, anti). ^{31}P NMR (162 MHz, CD_3CN) **δ** 152 (1P, s, gauche), 150 (1P, s, anti). IR in CH_2Cl_2 1859 and 1835 cm^{-1} (CO). Anal. Calcd for $[C_{13}H_{20}O_5PW]_2$: C, 33.14; H, 4.29; N, 0. Found C, 33.13; H, 4.17; N, 0. HRMS (ESI-HFX) m/z: $[M + H]^+$ Calcd for $[C_{13}H_{20}O_5PWH]_2$ 944.140; Found 944.114.

$[CpW(CO)_2P(Bu)_3]_2$. Preparation of $[CpW(CO)_2P(Bu)_3]_2$ was adapted from literature procedures of similar complexes.[14,15,24,27] In an inert atmosphere glovebox, $CpW(CO)_2P(Bu)_3H$ (0.0436 g, 0.0859 mmol, 1.03 equiv) and $(Ph_3C)_2$ (0.0405 g, 0.0832 mmol, 1 equiv) were combined in a 20 mL scintillation vial. The solids were then dissolved in 1.5 mL diethyl ether and stirred for 10 min at room temperature. A pink solid crashed out of solution and was collected via filtration. The solid was rinsed 3 times with diethyl ether and dried under vacuum for 30 mins to yield a pink solid (0.0203g, 0.0200 mmol, 24%). ^{1}H NMR (400 MHz, CD_3CN)) **δ** 5.03 (10H, s, gauche), 4.93 (10H, s, anti), 1.49 (24H, m, *J* = 14.4, 7.2 Hz gauche), 1.39 (24H, t, *J* = 14.6, 7.3 Hz anti), 1.27 (12H, m), 0.94 (18H, m). ^{31}P NMR (162 MHz, CD_3CN) **δ** 9.33 (1P, s, gauche), 7.38 (1P, s, anti). IR in CH_2Cl_2 1830 and 1810 cm^{-1} (CO). Anal. Calcd for $[C_{13}H_{20}O_5PW]_2$: C, 44.98; H, 6.37; N, 0. Found C, 44.82; H, 6.15; N, 0. HRMS (ESI-HFX) m/z: [M] Calcd for $[C_{19}H_{32}O_2PW]_2$ 1014.480; Found 1014.328.

$[CpW(CO)_2P(Cy)_3]_2$. Preparation of $[CpW(CO)_2P(Cy)_3]_2$ was adapted from literature procedures of similar complexes.[14,15,24,27] In an inert atmosphere glovebox, $CpW(CO)_2P(Cy)_3H$ (0.0497 g, 0.0848 mmol, 1.03 equiv) and $(Ph_3C)_2$ (0.0402 g, 0.0826 mmol, 1 equiv) were combined in a 20 mL scintillation vial. The solids were then dissolved in 3 mL diethyl ether and stirred for 45 min at room temperature. A purple-pink solid crashed out of solution and was collected via filtration.

The solid was rinsed 3 times with diethyl ether and dried under vacuum for 30 mins to yield a purple-pink solid (0.0369 g, 0.0315 mmol, 38%). $[CpW(CO)_2P(Cy)_3]_2$ is not soluble in acetonitrile and characterization is limited. Anal. Calcd for $[C_{25}H_{38}O_2PW]_2$: C, 51.30; H, 6.56; N, 0. Found C, 51.26; H, 6.38; N, 0. HRMS (ESI-HFX) m/z: [M] Calcd for $[C_{25}H_{38}O_2PW]_2$ 1170.732; Found 1170.425.

Results and Discussion

Synthesis and characterization of $CpW(CO)_2PR_3H$ complexes

Syntheses of $CpW(CO)_2PR_3H$ (PR_3 = $P(OEt)_3$, $P(Bu)_3$, $P(Cy)_3$) were adapted from literature reports of similar complexes, whereby[5,13,23,24] $CpW(CO)_3H$ is stirred with PR_3 at room temperature in pentane and PR_3 exchanges with one of the CO ligands, affording $CpW(CO)_2PR_3H$.

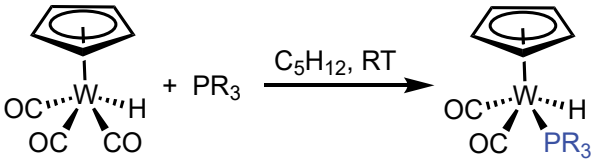

Scheme 2: Reaction scheme for the synthesis of $CpW(CO)s_2PR_3H$.

^1H NMR spectra of $CpW(CO)_2PR_3H$ H (PR_3 = $P(OEt)_3$ and $P(Cy)_3$) exhibit a diagnostic Cp resonance at room temperature that appears as a singlet at 5.39 and 5.36 ppm, respectively, along with a hydride resonance observed as a doublet at –8.25 and –7.64 ppm, respectively. A single phosphine resonance in the ^{31}P NMR is observed at 153 and 43.2 ppm for $P(OEt)_3$ and $P(Cy)_3$ respectively. Two Cp resonances are observed in the ^1H NMR spectrum of $CpW(CO)_2P(Bu)_3H$. The two Cp resonances in $CpW(CO)_2P(Bu)_3H$ are assigned to the cis and trans isomers of the complex at 5.35 and 5.17 ppm respectively, where cis and trans refer to the position of the phosphine relative to the hydride. The assignment of the two isomers is confirmed

by the presence of two diagnostic upfield metal hydride resonances observed as doublets in the ^{1}H NMR spectrum (–8.00 and –8.22 ppm) and two peaks in the ^{31}P NMR spectrum (14.1 and 7.36 ppm). Cis and trans isomers have distinct coupling constants for the metal hydride resonances coupling to the phosphorous, with a larger coupling constant observed for the cis configuration for molecules of the type $CpM(CO)_2PR_3H$.[28,29] Further investigation into PR_3 = $P(OEt)_3$ and $P(Cy)_3$, indicate coalescence of the isomers at room temperature. In low temperature ^{1}H NMR of PR_3 = $P(OEt)_3$, both isomers can be observed by ca. –10 °C and for PR_3 = $P(Cy)_3$, the peaks start to separate by ca. –30 °C, but the solvent freezes before the peaks are fully distinguishable (Figure S1, Table 1). Further, ^{183}W satellites are observed for the metal hydride complexes for PR_3 = $P(OEt)_3$ and $P(Bu)_3$.

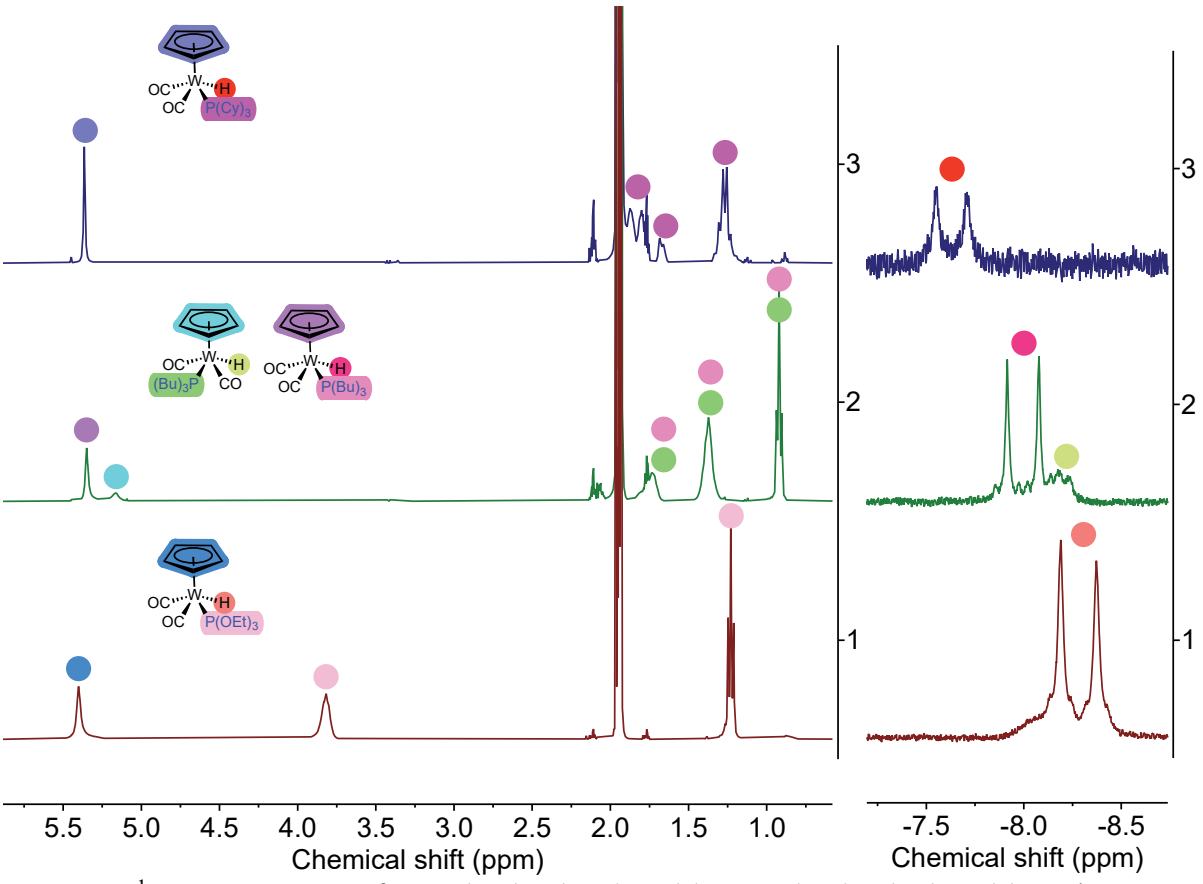

Figure 1: ^{1}H NMR spectra of $CpW(CO)_2P(OEt)_3H$ (1), $CpW(CO)_2P(Bu)_3H$ (2), and $CpW(CO)_2P(Cy)_3H$ (3) in CD_3CN acquired on a 400 MHz spectrometer. Peak assignments are color coded to the structures on the figure.

Table 1: ^{1}H NMR chemical shifts for Cp resonances, ^{1}H NMR chemical shifts for metal hydride resonances, coupling constants for the hydride peak of each complex by ^{1}H NMR, ^{31}P NMR chemical shifts of the PR_3 group, and the relative amounts of each isomer calculated by integration of the Cp resonance in the ^{1}H NMR spectra.

Compound/Temp.	**Isomer**	**Relative amount**	**Cp δ**	**Hydride δ (J_{PH})**
$CpW(CO)_2(P(OEt)_3)H$ ca. –30 °C	Cis	82%	5.41	–8.40 (72)
	Trans	18%	5.27	–8.08 (27)
$CpW(CO)_2(P(Bu)_3)H$ ca. 25 °C	Cis	72%	5.35	–8.00 (65.2)
	Trans	28%	5.17	–8.22 (23.0)
$CpW(CO)_2(P(Cy)_3)H$ ca. 25 °C	Cis/Trans Coalescence	–	5.36	-7.64 (60.9)

The cis and trans isomers of $CpW(CO)_2PR_3H$ are each expected to have two IR-active CO stretches based on their C_1 and C_s symmetries, respectively. However, the FTIR spectra of the $CpW(CO)_2PR_3H$ complexes in pentane only exhibit two CO stretches in the IR, 1955 and 1885 cm^{-1} ($P(OEt)_3$), 1939 and 1856 cm^{-1} ($P(Bu)_3$), 1934 and 1848 cm^{-1} ($P(Cy)_3$), indicating the isomers are likely of similar energy and their CO stretches overlap. In CH_2Cl_2, these CO stretches appear at 1941 and 1855 cm^{-1} ($P(OEt)_3$), 1918 and 1830 cm^{-1} ($P(Bu)_3$), and 1941 and 1856 cm^{-1} ($P(Cy)_3$).

Solutions of all the $CpW(CO)_2PR_3H$ complexes are pale yellow, and feature a broad absorption band in the UV region (Figure 2, $P(OEt)_3$ λ_{max} = 329 nm, ε = 1388 $M^{-1}cm^{-1}$; $P(Bu)_3$ λ_{max} = 347 nm ε = 1007 $M^{-1}cm^{-1}$; $P(Cy)_3$ λ_{max} = 350 nm ε = 979.5 $M^{-1}cm^{-1}$) of the UV-visible absorbance spectra. The transition is red shifted ca. 20 nm for the more donating phosphines $P(Bu)_3$ and $P(Cy)_3$.

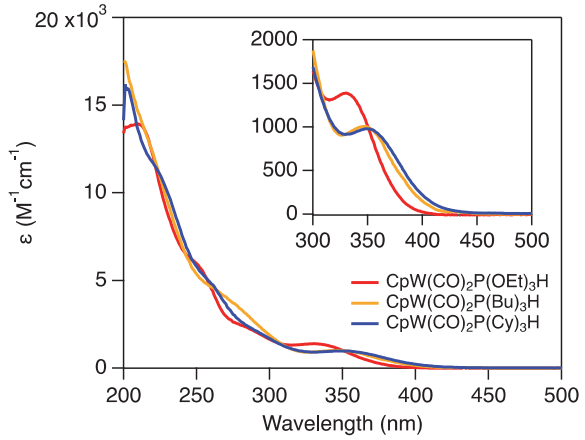

Figure 2: UV-vis absorbance spectra of $CpW(CO)_2P(OEt)_3H$ (red), $CpW(CO)_2P(Bu)_3H$ (orange), $CpW(CO)_2P(Cy)_3H$ (blue) in CH_3CN. Inset: Zoom-in of the features at ca. 350 nm.

Next, cyclic voltammetry and spectrophotometric titrations were utilized to characterize the thermochemical properties of the $CpW(CO)_2PR_3H$ complexes. These properties ultimately dictate the reagents necessary to promote the chemical transformations between $CpW(CO)_2PR_3H$ complexes and their PCET products highlighted in Scheme 1. Cyclic voltammograms of $CpW(CO)_2PR_3H$ contain a chemically irreversible oxidative wave, even at scan rates up to 10 V s^{-1} (Figure 3, Figures S2-4). Oxidation of $CpW(CO)_2PR_3H$ affords the unstable radical cation, $[CpW(CO)_2PR_3H]^{\bullet+}$, which can undergo a one-electron, one-proton PCET reaction and subsequently react with solvent to form $[CpW(CO)_2PR_3(CH_3CN)]^+$.[6,7] The anodic peak potentials range from 0.31 to 0.098 to 0.069 V vs $Fc^{+/0}$ for PR_3 = $P(OEt)_3$, $P(Bu)_3$, $P(Cy)_3$, respectively. This is in agreement with the Tolman electronic parameter ranking for the phosphine ligands derived from IR,[19] and indicates that $CpW(CO)_2PR_3H$ complexes are more readily oxidized with more donating ligands. These data fit the existing trend for known anodic peak potentials of $CpW(CO)_2LH$ complexes (L = CO, $P(Me)_3$, and IMes, where IMes = 1,3bis(2,4,6-trimethylphenyl)imidazol-2-ylidene). With L = CO, an anodic peak potential of 0.74 V vs $Fc^{+/0}$ was reported,[6,8,11] and as the ligand donor strength is increased, the peak shifts to more negative

potentials—anodic peak potentials of 0.16 V and –0.13 vs $Fc^{+/0}$ were recorded for L = $P(Me)_3$ [5,11] and L = IMes[7] respectively.

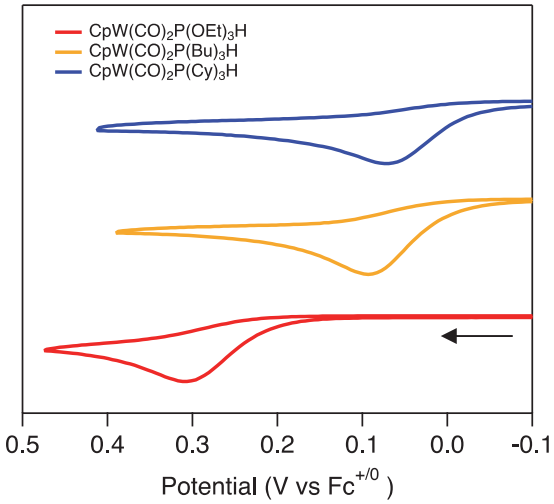

Figure 3: Cyclic voltammograms of $CpW(CO)_2P(OEt)_3H$ (0.74 mM, red), $CpW(CO)_2P(Bu)_3H$ (0.85 mM, orange), and $CpW(CO)_2P(Cy)_3H$ (0.31 mM, blue) in CH_3CN (250 mM $[NBu_4][PF_6]$) with a 50 mV s^{-1} scan rate and applied voltage corrected for ohmic drop using positive feedback R_u . Working electrode: glassy carbon, counter electrode: glassy carbon, reference electrode: silver wire pseudo electrode referenced to $Fc^{+/0}$ with ferrocene as an internal standard.

Understanding the acidity of $CpW(CO)_2PR_3H$ complexes guides the selection of appropriate bases to deprotonate the metal hydride complex to form $[CpW(CO)_2PR_3]^-$. Spectrophotometric titrations were performed to determine the pK_a values of the metal hydride complexes in this study (Figures 4, 5, S8–24).[30] As the electron donating ability of the phosphine increases, the pK_a value of the metal hydride complex increases. Experimental pK_a values were determined to be 25.4±0.1, 30.0±0.1, and 29.9±0.2 for PR_3 = $P(OEt)_3$, $P(Bu)_3$, and $P(Cy)_3$, respectively (values are the average of three trials). This presumably reflects the relatively stability of the conjugate base formed upon hydride deprotonation, $[CpW(CO)_2PR_3]^-$. These data fit existing trends for $CpW(CO)_2LH$ complexes; when L = CO a pK_a of 16,[6,8,11] L = $P(Me)_3$ has pK_a of 26.6, [5,11] and L = IMes has a pK_a of 32.9.[7] While the pK_a values of PR_3 = $P(Bu)_3$ and $P(Cy)_3$ fall

between those reported for $P(Me)_3$ and IMes, they are slightly higher than expected based on their relative donor strength compared to these previously reported complexes.

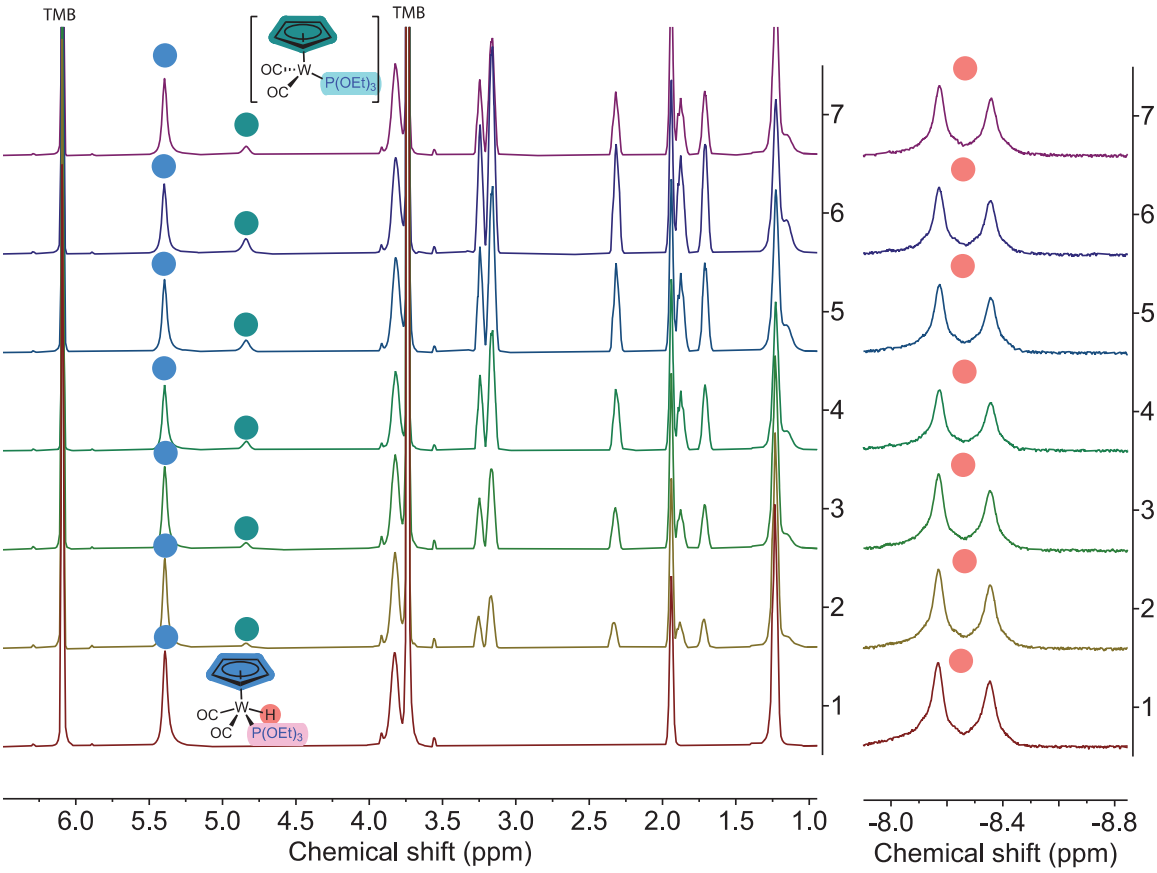

Figure 4: ^1H NMR spectra of $CpW(CO)_2P(OEt)_3H$ upon addition of 1, 5– diazabicyclo[4.3.0]non–5–ene (DBN). Spectra collected on a 400 MHz instrument in CD_3CN with 1, 3, 5 - trimethoxybenzene as an internal standard.

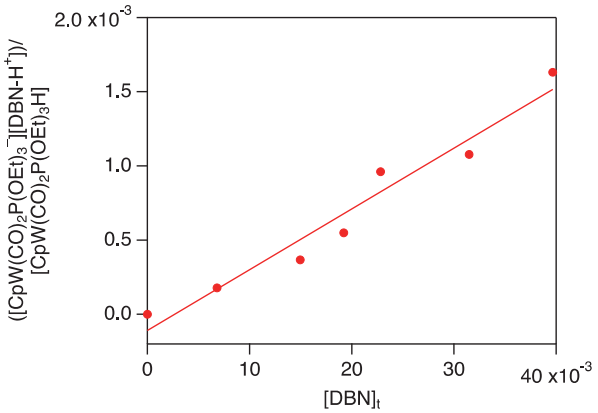

Figure 5: Plot of the relative concentrations of $[([CpW(CO)_2P(OEt)_3]^-][DBN–H^+])/[CpW(CO)_2P(OEt)_3H]$ vs $[DBN]_t$ (DBN = 1, 5– diazabicyclo[4.3.0]non–5–ene) Concentrations of $[CpW(CO)_2P(OEt)_3]^-$ and $CpW(CO)_2P(OEt)_3H$ were obtained by ^1H NMR spectroscopy with

reference to an internal standard, biphenyl. The linear fit of the plot is y = 0.0369x – 0.000188 with an r^2 value of 0.9688. This plot represents the first trial of the three trials conducted. The pK_a value in the main text is the average of three trials.

Synthesis and characterization of [Na][CpW(CO)$_2$PR$_3$] complexes

The syntheses of [Na][CpW(CO)$_2$PR$_3$] complexes were adapted from literature procedure.[5,16,24] First, CpW(CO)$_2$PR$_3$H was combined with excess NaH and stirred overnight in acetonitrile. Then, excess NaH was removed via filtration to isolate [Na][CpW(CO)$_2$PR$_3$].

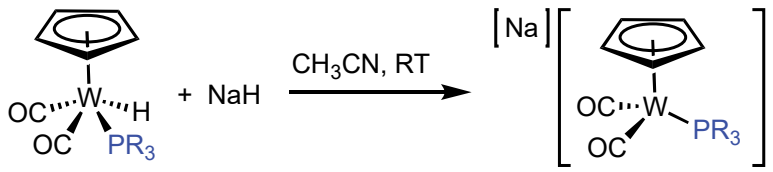

Scheme 3: Reaction scheme for the synthesis of [Na][CpW(CO)$_2$PR$_3$].

Successful synthesis of [Na][CpW(CO)$_2$PR$_3$] is supported by ^{1}H NMR spectra (Figure 6), in which the up field metal hydride peak observed in spectra of CpW(CO)$_2$PR$_3$H is absent. The Cp peak is upfield relative to that of the corresponding neutral metal hydride species, at 4.84, 4.70, and 4.70 ppm for PR$_3$ = P(OEt)$_3$, P(Bu)$_3$, and P(Cy)$_3$, respectively (Figure 6). The ^{31}P NMR contains a single phosphorous peak at 177, 21.6, and 43.1 ppm for PR$_3$ = P(OEt)$_3$, P(Bu)$_3$, and P(Cy)$_3$, respectively.

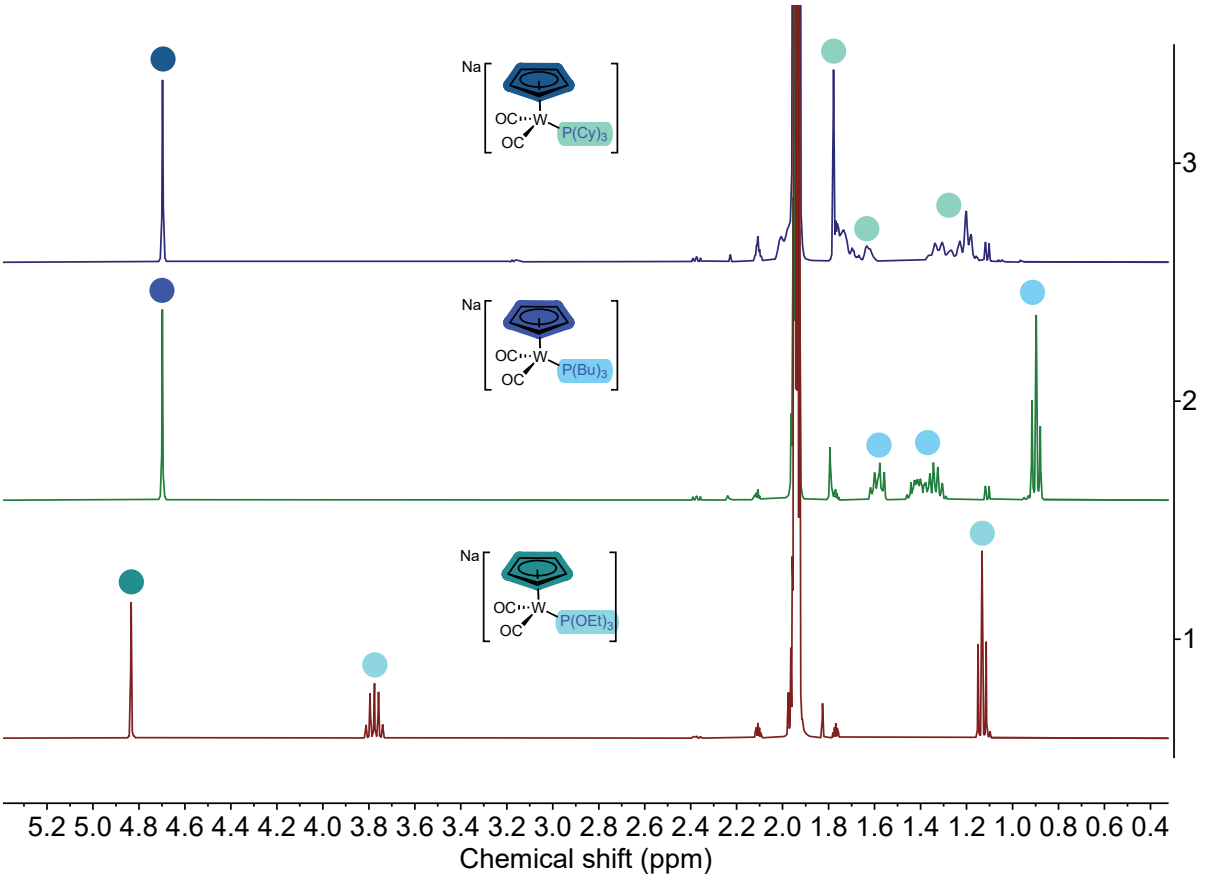

Figure 6: The ^{1}H NMR spectra of [Na][CpW(CO)$_2$P(OEt)$_3$] (1), [Na][CpW(CO)$_2$P(Bu)$_3$] (2), and [Na][CpW(CO)$_2$P(Cy)$_3$] (3) in CD$_3$CN acquired on a 400 MHz spectrometer. Peak assignments are color coded to the structures on the figure.

The FTIR spectra of [Na][CpW(CO)$_2$PR$_3$] each contain two CO stretches, as predicted based on their C_s symmetry. Surprisingly, the frequencies of the CO stretches in CH_2Cl_2 are very similar across PR$_3$ = P(OEt)$_3$, P(Bu)$_3$, and P(Cy)$_3$ at 1942 and 1848 cm^{-1}; 1937 and 1844 cm^{-1}; and, 1937 and 1848 cm^{-1} respectively, and do not trend with the electronics of the phosphine.[19]

Solutions of the [Na][CpW(CO)$_2$PR$_3$] complexes are yellow. The UV-visible absorption profile for all analogs contains an intense transition at 253 nm (ε = 1236 M^{-1}cm^{-1}), 248 nm (ε = 1446 M^{-1}cm^{-1}) 253 nm (ε = 4512 M^{-1}cm^{-1}), and a shoulder around 300-350 nm for PR$_3$ = P(OEt)$_3$, P(Bu)$_3$, and P(Cy)$_3$ respectively (Figure 7). While the absorbance feature appears at similar energy for all three complexes, the extinction coefficient for the P(Cy)$_3$ complex is much larger than the

other analogues. In addition, the peak at 253 nm is more pronounced for $P(Cy)_3$, while the 253 nm and the 248 nm peaks for $P(OEt)_3$, $P(Bu)_3$ respectively, appear as a shoulder rather than a distinct peak. The cause of this difference in peak shape is unclear and more studies are needed to determine its origin.

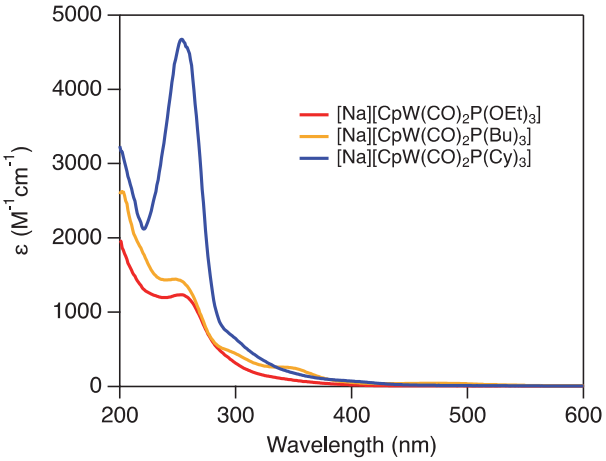

Figure 7: UV-vis absorbance spectra of $[Na][CpW(CO)_2P(OEt)_3]$ (red), $[Na][CpW(CO)_2P(Bu)_3]$ (orange), $[Na][CpW(CO)_2P(Cy)_3]$ (blue) in CH_3CN.

Similar to the $CpW(CO)_2PR_3H$ complexes, electrochemistry can provide insight into the PCET reactivity of these complexes. The cyclic voltammograms of $[Na][CpW(CO)_2PR_3]$ recorded at 50 mV/s contain a chemically irreversible oxidative wave that is attributed to the oxidation of $[Na][CpW(CO)_2PR_3]$ to $[CpW(CO)_2PR_3]^{\bullet}$, which can undergo further oxidation and solvent association to form $[CpW(CO)_2PR_3(CH_3CN)]^+$ or dimerize to form $[CpW(CO)_2PR_3]_2$.[5–7] (Figure 8, Figures S5-7, Scheme 1). The anodic peak potential shifts to more negative potentials as the electron donating ability of the phosphine is increased from –0.95 to –1.23 to –1.26 V vs $Fc^{+/0}$ for $PR_3 = P(OEt)_3$, $P(Bu)_3$, and $P(Cy)_3$ respectively, consistent with trends observed for oxidation of $CpW(CO)_2PR_3H$. For $PR_3 = P(Cy)_3$, the oxidation of $[Na][CpW(CO)_2PR_3]$ to $[CpW(CO)_2 PR_3]^{\bullet}$ becomes reversible as the scan rate is increased from 50 to 10,000 mV/s. We hypothesize that the kinetics of dimerization are substantially slower for $PR_3 = P(Cy)_3$ as compared to $PR_3 = P(OEt)_3$

and $P(Bu)_3$, due to steric bulk of the ligand, such that at faster scan rates the species can be reduced before dimerization occurs.

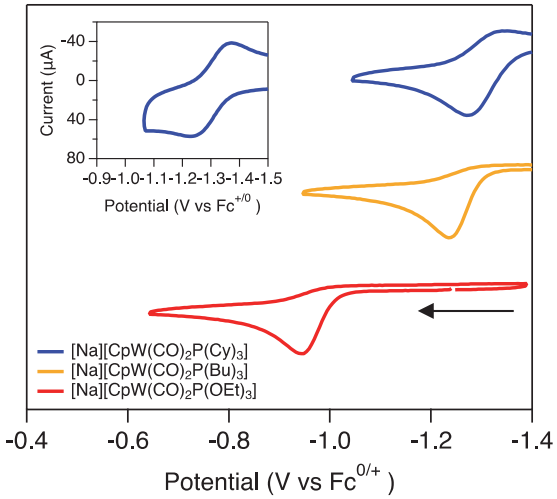

Figure 8: Cyclic voltammograms of $Na[CpW(CO)_2P(OEt)_3]$ (0.73 mM, red), $Na[CpW(CO)_2P(Bu)_3]$ (0.74 mM, orange), and $Na[CpW(CO)_2P(Cy)_3]$ (0.60 mM, blue) in CH_3CN (250 mM $[NBu_4][PF_6]$) with a 50 mV s^{-1} scan rate and corrected for IR compensation. Working electrode: glassy carbon, counter electrode: glassy carbon, reference electrode: silver wire pseudo electrode referenced to $Fc^{+/0}$ with ferrocene as an internal standard. Inset: Voltammogram of 0.60 mM $Na[CpW(CO)_2P(Cy)_3]$ recorded at 7500 mVs^{-1}.

Synthesis and characterization of $[CpW(CO)_2PR_3(CH_3CN)][PF_6]$ complexes

The syntheses of the $[CpW(CO)_2PR_3(CH_3CN)][PF_6]$ complexes were adapted from literature procedures.[11,14,24,26] $CpW(CO)_2PR_3H$ was combined with trityl hexafluorophosphate and five equivalents of CH_3CN, then stirred at room temperature. The solvent was removed by vacuum and the byproduct, Ph_3CH was extracted with diethyl ether yielding $[CpW(CO)_2PR_3(CH_3CN)][PF_6]$.

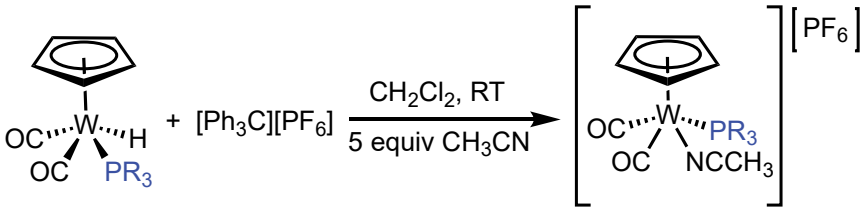

Scheme 4: Reaction scheme for the synthesis of $[CpW(CO)_2PR_3(CH_3CN)][PF_6]$.

In the ^{1}H NMR spectra (Figure 9), the Cp peak is shifted downfield compared to the metal hydride complexes, appearing at 5.59, 5.80, and 5.86 ppm for PR_3 = $P(OEt)_3$, $P(Bu)_3$, and $P(Cy)_3$ respectively. Additionally, a new peak at ca. 2.5 ppm is observed, characteristic of a bound CH_3CN ligand. Two CO stretches are observed in the IR spectra of these complexes in CH_2Cl_2 at 1912 and 1998 cm^{-1} for PR_3 = $P(OEt)_3$, 1889 and 1974 cm^{-1} for PR_3 = $P(Bu)_3$; and 1889 and 1971 cm^{-1} for PR_3 = $P(Cy)_3$. Cis and trans isomers are possible for $[CpW(CO)_2PR_3(CH_3CN)][PF_6]$ complexes, but the isomers appear to be indistinguishable at room temperature by both NMR and FTIR.

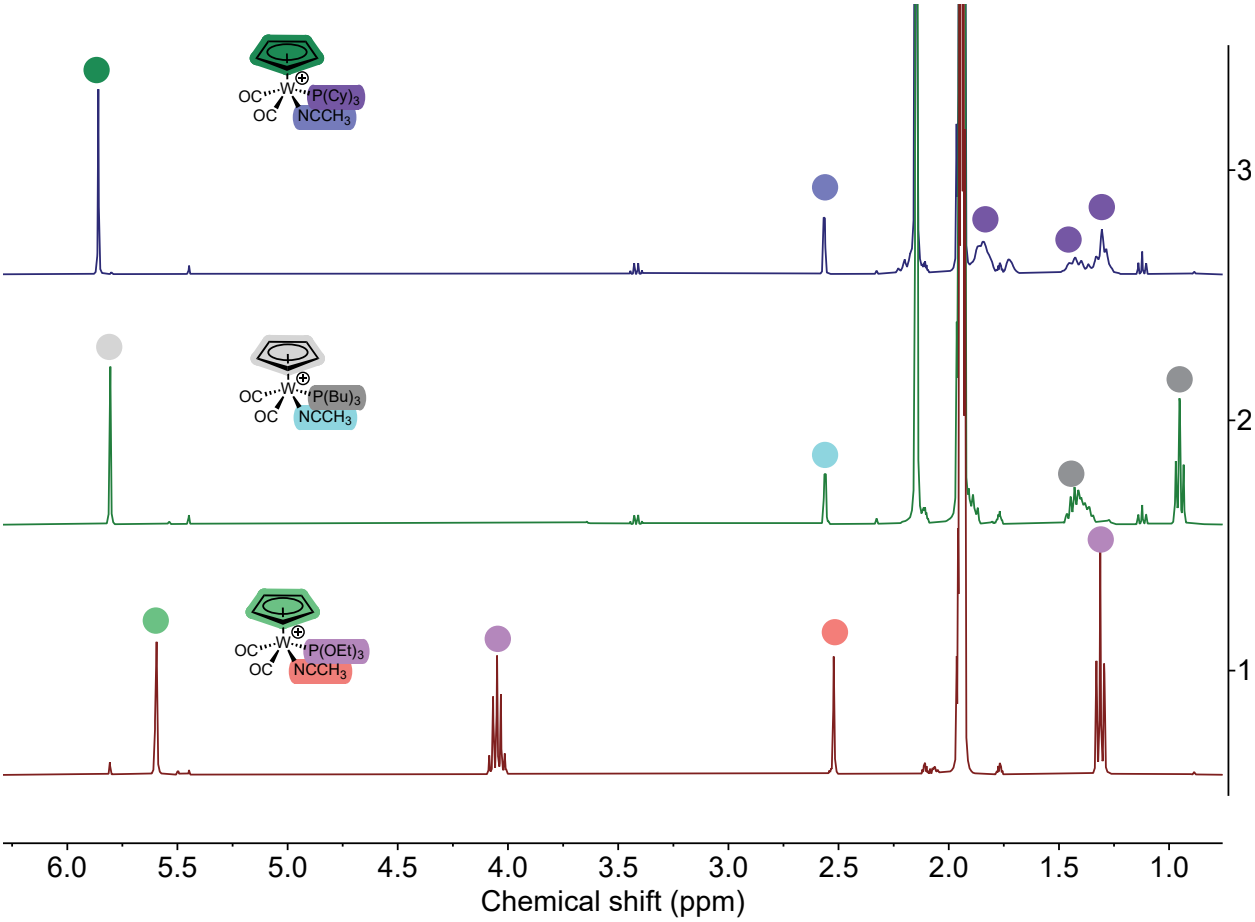

Figure 9: The ^{1}H NMR spectra of $[CpW(CO)_2P(OEt)_3(CH_3CN)][PF_6]$ (1), $[CpW(CO)_2P(Bu)_3(CH_3CN)][PF_6]$ (2), and $[CpW(CO)_2P(Cy)_3(CH_3CN)][PF_6]$ (3) in CD_3CN acquired on a 400 MHz spectrometer. Peak assignments are color coded to the structures on the figure.

Solutions of the $[CpW(CO)_2PR_3(CH_3CN)][PF_6]$ complexes in acetonitrile are orange, with a broad absorption bands (Figure 10, $P(OEt)_3$ λ_{max} = 413 nm, ε = 741 M^{-1}cm^{-1}; $P(Bu)_3$ λ_{max} = 405

nm ε = 891 $M^{-1}cm^{-1}$; $P(Cy)_3$ λ_{max} = 432 nm ε = 589 $M^{-1}cm^{-1}$). There is a minimal peak shift of less than 30 nm between the analogs, with the $P(Cy)_3$ complex absorbing furthest to the red.

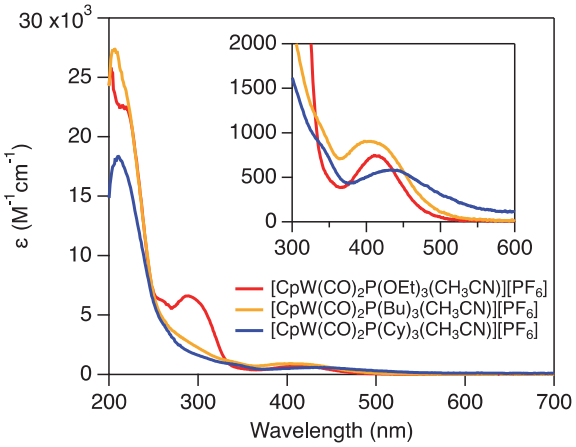

Figure 10: UV-vis absorbance spectra of $[CpW(CO)_2P(OEt)_3(CH_3CN)][PF_6]$ (red), $[Na][CpW(CO)_2P(Bu)_3(CH_3CN)][PF_6]$ (orange), $[Na][CpW(CO)_2P(Cy)_3(CH_3CN)][PF_6]$ (blue) in CH_3CN.

Synthesis and characterization of $[CpW(CO)_2PR_3]_2$ Complexes

The syntheses of $[CpW(CO)_2PR_3]_2$ complexes were adapted from literature procedures.[14,15,24,27] $CpW(CO)_2PR_3H$ was combined with Gomberg's dimer ($(Ph_3C)_2$) and stirred at room temperature in diethyl ether to afford $[CpW(CO)_2PR_3]_2$, which is isolated through filtration. This reaction occurs through H atom abstraction to form Ph_3CH and $[CpW(CO)_2PR_3]^{\bullet}$ which subsequently dimerizes to form $[CpW(CO)_2PR_3]_2$.

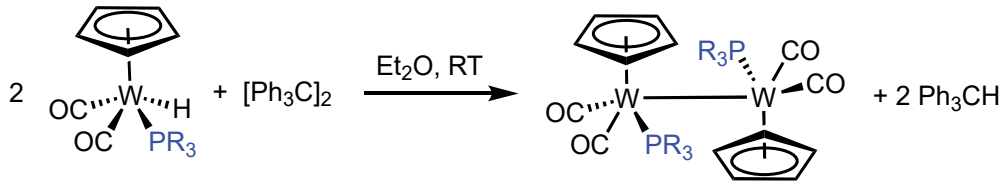

Scheme 5: Reaction scheme for the synthesis of $[CpW(CO)_2PR_3]_2$.

Due to solubility issues, we were unable to fully characterize $[CpW(CO)_2P(Cy)_3]_2$. $[CpW(CO)_2P(OEt)_3]_2$ and $[CpW(CO)_2P(Bu)_3]_2$, both contain anti and gauche isomers with the possibility of more complex isomerization, such as accounting for any cis and trans isomers in

addition to anti and gauche isomers. The presence of anti and gauche isomers is indicated by a pair of resonances for the Cp protons at 5.13 and 5.05 ppm for $PR_3 = P(OEt)_3$ and 5.03 and 4.93 for $PR_3 = P(Bu)_3$ (Figure 11, Table S1). Similar complexes in the literature are also reported to form as a mixture of both the anti and gauche isomers.[14,15,24,27] In the IR spectra in CH_2Cl_2 there are two peaks in the carbonyl region at 1859 and 1835 cm^{-1} for $PR_3 = P(OEt)_3$ and 1830 and 1810 cm^{-1} for $PR_3 = P(Bu)_3$. While there are at least two isomers present and there are two stretches predicted for each isomer, only two stretches are observed, the isomers are likely of similar energy and their CO stretches overlap resulting in only two stretches.

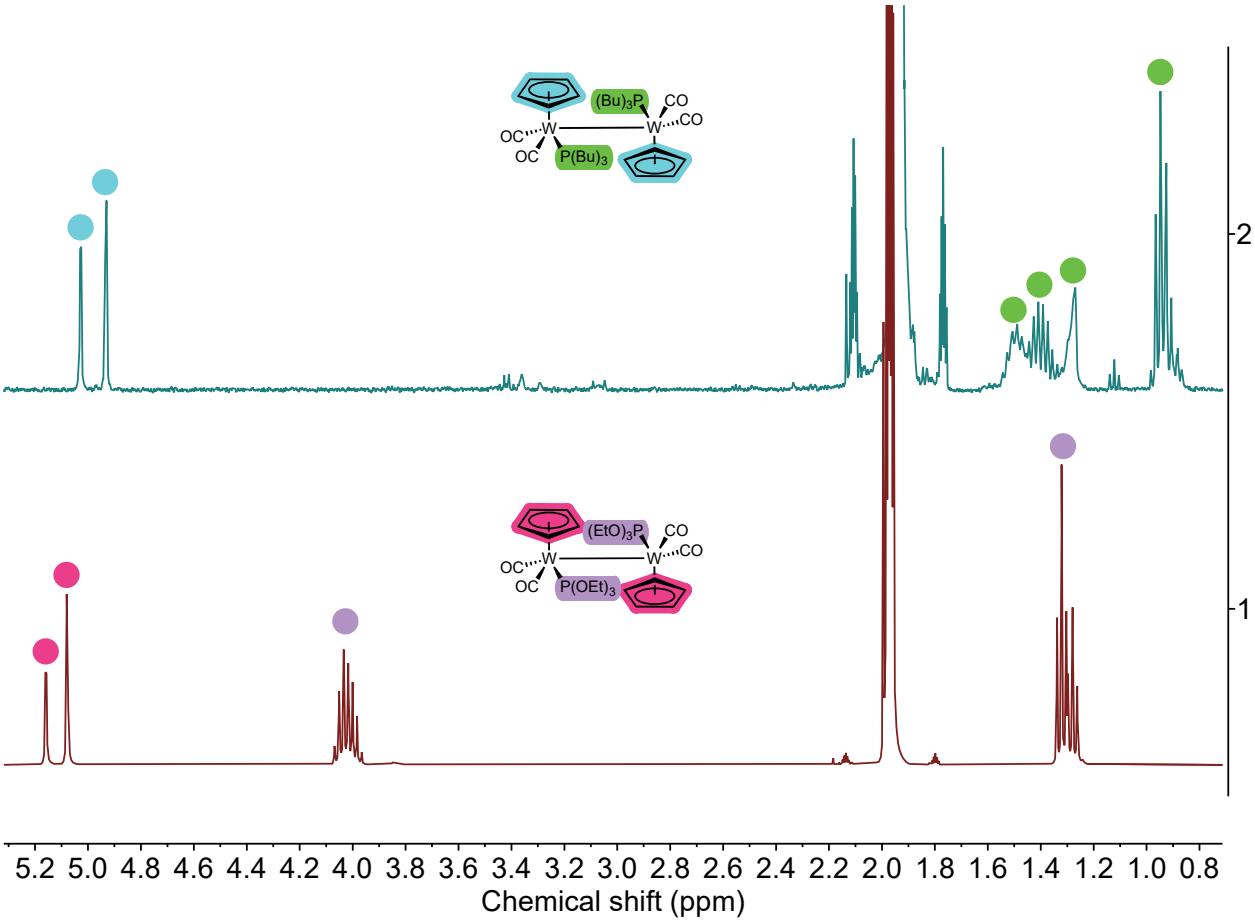

Figure 11: The ^1H NMR spectra of $[CpW(CO)_2P(OEt)_3]_2$ (1), $[CpW(CO)_2P(Bu)_3]_2$ (2)) in CD_3CN acquired on a 400 MHz spectrometer. Peak assignments are color coded to the structures on the figure.

The UV-visible absorbance spectra of the $[CpW(CO)_2PR_3]_2$ complexes contain two absorption features . The first is an intense absorption band between 300–400 nm and is attributed to $\sigma \rightarrow \sigma^*$ transition.[24,31] A second less intense broad band is observed 425–550 nm that is attributed to the $d\pi \rightarrow \sigma^*$ transition (Figure 12).[24,31] The absorption features are red-shifted for the more electron donating phosphine, $P(Bu)_3$ complex (350 nm, ε = 11166 $M^{-1}cm^{-1}$; 483 nm, ε = 1676 $M^{-1}cm^{-1}$) compared to the more electron withdrawing phosphine, $P(OEt)_3$ species (345 nm, ε = 18665 $M^{-1}cm^{-1}$; 473 nm, ε = 2257 $M^{-1}cm^{-1}$), similar to what was observed in the UV-visible absorption spectra of the $CpW(CO)_2PR_3H$ complexes. For $PR_3 = P(Cy)_3$ complex (355 nm, 502 nm), similar features are observed in toluene, but the complex is only sparingly soluble and therefore the measurement is purely qualitative (Figure S24).

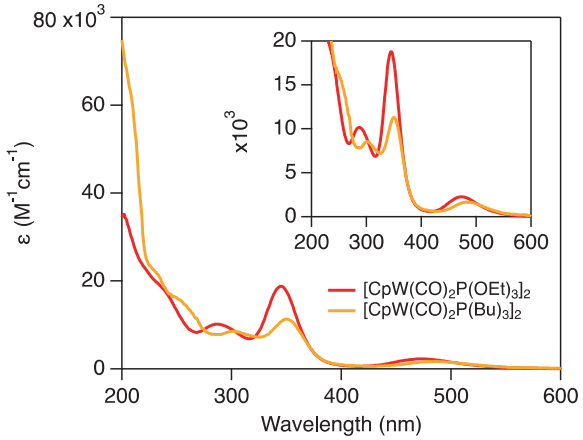

Figure 12: UV-vis spectra of $[CpW(CO)_2P(OEt)_3]_2$ (red), and $CpW(CO)_2P(Bu)_3]_2$ (orange) in CH_3CN.

Conclusion

A series of $CpW(CO)_2PR_3H$ (PR_3 = $P(OEt)_3$, $P(Bu)_3$, and $P(Cy)_3$), $[CpW(CO)_2PR_3]^-$, $[CpW(CO)_2PR_3(CH_3CN)]^+$, and $[CpW(CO)_2PR_3]_2$ complexes were synthesized to examine the influence of the steric and the electronic parameters of the phosphine ligands on the complexes thermochemical properties. These complexes were characterized by ^1H NMR, IR, and UV-visible absorbance spectroscopy where it was found that the phosphine electronics impact the

thermochemical properties of these complexes, aligning with existing trends known about electron donating abilities of these phosphines. In ^{1}H NMR spectra, the Cp peaks shift upfield for the more electron donating phosphines due to the increased electron density on the metal center that increases shielding. The UV-visible absorbance features show minimal shifts in absorbance features (less than 50 nm) between analogs; where the more electron donating phosphine complexes are red shifted.

The cyclic voltammograms of the $CpW(CO)_2PR_3H$ and $[CpW(CO)_2PR_3]^-$ complexes further inform on the influence of PR_3 on the electronics and kinetics of these tungsten complexes. The $E_{p,a}(CpW(CO)_2PR_3H^{+/0})$ and $E_{p,a}(CpW(CO)_2PR_3{}^{0/-})$ values shift anodically as the donor ability of PR_3 is decreased. Furthermore, reversibility of the $CpW(CO)_2PR_3{}^{0/-}$ couple is regained for $PR_3 = P(Cy)_3$ as scan rate is increased, as the dimerization kinetics of the radical species are attenuated with the sterically bulky $P(Cy)_3$ phosphine. The pK_a values of the $CpW(CO)_2PR_3H$ complexes, measured via spectrophotometric titration, increase with donor strength of the PR_3 Ligand. The trends of these data indicates the electron donating ability of the phosphine increases from $P(OEt)_3$ to $P(Bu)_3$ to $P(Cy)_3$, which is in good agreement with the Tolman electronic parameter for these phosphines.[19] The synthesis and characterization of $CpW(CO)_2PR_3H$, $[CpW(CO)_2PR_3]^-$, $[CpW(CO)_2\ PR_3(CH_3CN)]^+$, and $[CpW(CO)_2PR_3]_2$ species reported in this work will allow researchers to better identify and understand electron, proton, and proton-coupled electron transfer reactivity of these complexes.

Supporting Information. The following files are available free of charge. Additional characterization details, electrochemical data, and spectrophotometric titration plots.

Corresponding Author

Jillian L. Dempsey – *Department of Chemistry, University of North Carolina at Chapel Hill, Chapel Hill, North Carolina 27599-3290, United States.* http://orcid.org/0000-0002-9459-4166; Email: dempseyj@email.unc.edu

ACKNOWLEDGMENT

This work was supported by the National Science Foundation (CHE-1954868). J.L.D. acknowledges support from a Packard Fellowship for Science and Engineering. We thank Joseph Templeton for insightful discussions on NMR coupling constants. We thank the University of North Carolina's Department of Chemistry NMR Core Laboratory for the use of their NMR spectrometers. We thank the University of North Carolina's Department of Chemistry Mass Spectrometry Core Laboratory, especially Lazaro Toledo Machin, for their assistance with mass spectrometry analysis. This work made use of an NMR spectrometer (CHE-0922858) and a mass spectrometer (CHE-1726291) supported by the National Science Foundation.

References

[1] Perutz, R. N.; Procacci, B. Photochemistry of Transition Metal Hydrides. *Chemical Reviews* **2016**, *116* (15), 8506–8544. https://doi.org/10.1021/acs.chemrev.6b00204.

[2] Concepcion, J. J.; House, R. L.; Papanikolas, J. M.; Meyer, T. J. Chemical Approaches to Artificial Photosynthesis. *Proceedings of the National Academy of Sciences of the United States of America* **2012**, *109* (39), 15560–15564. https://doi.org/10.1073/pnas.1212254109.

[3] Lennox, J. C.; Kurtz, D. A.; Huang, T.; Dempsey, J. L. Excited-State Proton-Coupled Electron Transfer: Different Avenues for Promoting Proton/Electron Movement with Solar Photons. *ACS Energy Letters* **2017**, *2* (5), 1246–1256. https://doi.org/10.1021/acsenergylett.7b00063.

[4] Whittemore, T. J.; Xue, C.; Huang, J.; Gallucci, J. C.; Turro, C. Single-Chromophore Single-Molecule Photocatalyst for the Production of Dihydrogen Using Low-Energy Light. *Nature Chemistry* **2020**, *12*, 180–185. https://doi.org/10.1038/s41557-019-0397-4.

[5] Huang, T.; Rountree, E. S.; Traywick, A. P.; Bayoumi, M.; Dempsey, J. L. Switching between Stepwise and Concerted Proton-Coupled Electron Transfer Pathways in Tungsten Hydride Activation. *J. Am. Chem. Soc* **2018**, *140*, 14655–14669. https://doi.org/10.1021/jacs.8b07102.

[6] Bourrez, M.; Steinmetz, R.; Ott, S.; Gloaguen, F.; Hammarström, L. Concerted Proton-Coupled Electron Transfer from a Metal-Hydride Complex. *Nature Chemistry* **2015**, *7* (2), 140–145. https://doi.org/10.1038/nchem.2157.

[7] Roberts, J. A. S.; Appel, A. M.; DuBois, D. L.; Bullock, R. M. Comprehensive Thermochemistry of W–H Bonding in the Metal Hydrides $CpW(CO)_2(IMes)H$, $[CpW(CO)_2(IMes)H]^{\bullet+}$, and $[CpW(CO)_2(IMes)(H)_2]^+$. Influence of an N-Heterocyclic Carbene Ligand on Metal Hydride Bond Energies. *J. Am. Chem. Soc.* **2011**, *133* (37), 14604–14613. https://doi.org/10.1021/ja202830w.
[8] Liu, T.; Guo, M.; Orthaber, A.; Lomoth, R.; Lundberg, M.; Ott, S.; Hammarström, L. Accelerating Proton-Coupled Electron Transfer of Metal Hydrides in Catalyst Model Reactions. *Nature Chemistry* **2018**, *10* (8), 881–887. https://doi.org/10.1038/s41557-018-0076-x.
[9] Liu, T.; Tyburski, R.; Wang, S.; Fernández-Terán, R.; Ott, S.; Hammarström, L. Elucidating Proton-Coupled Electron Transfer Mechanisms of Metal Hydrides with Free Energy- and Pressure-Dependent Kinetics. *J. Am. Chem. Soc.* **2019**, *141* (43), 17245–17259. https://doi.org/10.1021/jacs.9b08189.
[10] Kristjansdottir, S. S.; Moody, A. E.; Weberg, R. T.; Norton, J. R. Kinetic and Thermodynamic Acidity of Hydrido Transition-Metal Complexes. 5. Sensitivity of Thermodynamic Acidity to Ligand Variation and Hydride Bonding Mode. *Organometallics* **1988**, *7* (9), 1983–1987. https://doi.org/10.1021/om00099a013.
[11] Ryan, O. B.; Tilset, M.; Parker, V. D. Chemical and Electrochemical Oxidation of Group 6 Cyclopentadienylmetal Hydrides. First Estimates of 17-Electron Metal Hydride Cation Radical Thermodynamic Acidities and Their Decomposition to 17-Electron Neutral Radicals. *J. Am. Chem. Soc* **1990**, *112* (1), 2618–2626. https://doi.org/10.1021/ja00163a023.
[12] Parker, V. D.; Tilset, M. Solution Homolytic Bond Dissociation Energies of Organotransition-Metal Hydrides. *J. Am. Chem. Soc* **1989**, *111* (17), 6711–6717. https://doi.org/10.1021/ja00199a034.
[13] Kalck, P.; Pince, R.; Poilblanc, R.; Roussel, J. Study of the Exchange Phenomenon between Two Isomers of Phosphine Substituted Carbonyl-π-Cyclopentadienyl Complexes of Molybdenum and Tungsten II. Steric Influence of Bulky Groups in Phosphines. *Journal of Organometallic Chemistry* **1970**, *24* (2), 445–452. https://doi.org/10.1016/S0022-328X(00)80287-9.
[14] Tilset, M. Oxidation of $CpM(CO)_3^{\bullet}$ and $CpM(CO)_3(NCMe)^{\bullet}$ (M = Cr, Mo, W): Kinetic and Thermodynamic Considerations of Their Possible Involvement as Reducing Agents. Relative Acetonitrile Affinities of $CpM(CO)_3^+$ and $CpM(CO)_3^{\bullet}$. *Inorganic Chemistry* **1994**, *33* (14), 3121–3126. https://doi.org/10.1021/ic00092a018.
[15] Van Der Eide, E. F.; Yang, P.; Walter, E. D.; Liu, T.; Bullock, R. M. Dinuclear Metalloradicals Featuring Unsupported Metal-Metal Bonds. *Angewandte Chemie - International Edition* **2012**, *51* (33), 8361–8364. https://doi.org/10.1002/anie.201203531.
[16] Patil, H. R. H.; Graham, W. A. G. Organometallic Compounds with Metal-Metal Bonds. I. Tricarbonyl-π-Cyclopentadienylchromium, -Molybdenum, and -Tungsten Bonded to Methyl and Phenyl Derivatives of Germanium, Tin, and Lead. *Inorganic Chemistry* **1966**, *5* (8), 1401–1405. https://doi.org/10.1021/ic50042a026
[17] Roberts, J. A. S.; DuBois, D. L.; Bullock, R. M. Experimental and Digital Simulation Studies of the Electrochemical Oxidation of the Metal Anion $[CpW(CO)_2(IMes)]^-$ and the 17-Electron Metal Radical $CpW(CO)_2(IMes)^{\bullet}$. Kinetics and Thermodynamics of Capture and Release of MeCN by a Metal Radical and a Metal Cation. *Organometallics* **2011**, *30* (17), 4555–4563. https://doi.org/10.1021/om2002816.

[18] Bullock, R. M.; Song, J.-S.; Szalda, D. J. Protonation of Metal Hydrides by Strong Acids. Formation of an Equilibrium Mixture of Dihydride and Dihydrogen Complexes from Protonation of Cp*Os(CO) $_2$ H. Structural Characterization of $[CpW(CO)_2(PMe_3)(H)_2]^+$ OTf $^-$. *Organometallics* **1996**, *15* (10), 2504–2516. https://doi.org/10.1021/om950976y.
[19] Tolman, C. A. Electron Donor-Acceptor Properties of Phosphorus Ligands. Substituent Additivity. *J. Am. Chem. Soc.* **1970**, *92* (10), 2953–2956. https://doi.org/10.1021/ja00713a006.
[20] Jover, J.; Cirera, J. Computational Assessment on the Tolman Cone Angles for P-Ligands. *Dalton Transactions* **2019**, *48*, 15036–15048. https://doi.org/10.1039/c9dt02876e.
[21] Tolman, C. A. Phosphorus Ligand Exchange Equilibriums on Zerovalent Nickel. Dominant Role for Steric Effects. *J. Am. Chem. Soc.* **1970**, *92* (10), 2956–2965. https://doi.org/10.1021/ja00713a007.
[22] Hoffman, N. W.; Brown, T. L. Thermal and Photochemical Substitution Reactions of the Tricarbonyl(Cyclopentadienyl)Hydrido Compounds of Tungsten and Molybdenum. *Inorg. Chem.* **1978**, *17* (3), 613–617. https://doi.org/10.1021/ic50181a019.
[23] Li, C.; Gao, F.; Cheng, S.; Tjahjono, M.; Van Meurs, M.; Tay, B. Y.; Jacob, C.; Guo, L.; Garland, M. From Stoichiometric to Catalytic Binuclear Elimination in Rh-W Hydroformylations. Identification of Two New Heterobimetallic Intermediates. *Organometallics* **2011**, *30* (16), 4292–4296. https://doi.org/10.1021/om200306j.
[24] Isaacs, D. P.; Gruninger, C. T.; Huang, T.; Jordan, A. M.; Nicholas, G.; Chen, C.-H.; Horst, M. A. ter; Dempsey, J. L. Visible Light Induced Formation of a Tungsten Hydride Complex. *Dalton Trans.* **2023**, *52* (10), 3210–3218. https://doi.org/10.1039/D2DT03675D.
[25] Cheng, T. Y.; Szalda, D. J.; Zhang, J.; Bullock, R. M. Synthesis and Structure of CpMo(CO)(Dppe)H and Its Oxidation by Ph_3C^+. *Inorganic Chemistry* **2006**, *45* (12), 4712–4720. https://doi.org/10.1021/ic060111k.
[26] Gibson, D. H.; Owens, K.; Mandal, S. K.; Sattich, W. E.; Franco, J. O. Synthesis and Thermolysis of Neutral Metal Formyl Complexes of Molybdenum, Tungsten, Manganese, and Rhenium. *Organometallics* **1989**, *8*, 498–505. https://doi.org/10.1021/om00104a035
[27] Barbini, D. C.; Tanner, P. S.; Francone, T. D.; Furst, K. B.; Jones, W. E. Direct Electrochemical Investigations of 17-Electron Complexes of $CpM(CO)_3^{\bullet}$ (M = Mo, W, and Cr). *Inorganic Chemistry* **1996**, *35* (13), 4017–4022. https://doi.org/10.1021/ic951303a.
[28] Faller, J. W.; Anderson, A. S. Organometallic Conformational Equilibria. XI. Isomerism and Stereochemical Nonrigidity in Cyclopentadienylmolybdenum Complexes. *Journal of the American Chemical Society* **1970**, *92* (20), 5852–5860. https://doi.org/10.1021/ja00723a007.
[29] King, R. B.; Pannell, K. H. Complexes of Trivalent Phosphorus Derivatives. VII. Some Triphenyl Phosphite Derivatives of Cyclopentadienylmolybdenum Carbonyls. *Inorg. Chem.* **1968**, *7* (11), 2356–2361. https://doi.org/10.1021/ic50069a035.
[30] Saouma, C. T.; Kaminsky, W.; Mayer, J. M. Protonation and Concerted Proton–Electron Transfer Reactivity of a Bis-Benzimidazolate Ligated [2Fe–2S] Model for Rieske Clusters. *J. Am. Chem. Soc.* **2012**, *134* (17), 7293–7296. https://doi.org/10.1021/ja3019324.
[31] Wrighton, M. S.; Ginley, D. S. Photochemistry of Metal-Metal Bonded Complexes. III. Photoreactivity of Hexacarbonylbis(η5-Cyclopentadienyl)Dimolybdenum(I) and -Ditungsten(I). *J. Am. Chem. Soc* **1975**, *97* (15), 4246–4251. https://doi.org/10.1021/ja00848a016.